Analog Complex Gammatone Filter for Cochlear Implant Channels

Wannaya Ngamkham, Chutham Sawigun, Senad Hiseni and Wouter A. Serdijn

Biomedical Electronics Group, Electronics Research Laboratory, Delft University of Technology, the Netherlands
w.ngamkham@tudelft.nl, c.sawigun@tudelft.nl, senad.hiseni@gmail.com and w.a.serdijn@tudelft.nl

***Abstract*— According to recent physiological experiments, the envelope and phase of speech signals are required to enhance the perceptive capability of a cochlear implant processor. In this paper, the design of an analog complex gammatone filter is introduced in order to extract both envelope and phase information of the incoming speech signals as well as to emulate the basilar membrane spectral selectivity. The gammatone impulse response is first transformed into the frequency domain and the resulting 8th-order transfer function is subsequently mapped onto a state-space description of an orthonormal ladder filter. Using this approach, the real and imaginary transfer functions that share the same denominator can be extracted using two different C matrices. This results in a compact filter structure. The proposed filter is designed using G_m-C integrators and sub-threshold CMOS devices in AMIS 0.35μm technology. Simulation results using Cadence RF Spectre confirm the design principle and ultra low power operation.**

I. INTRODUCTION

Cochlear Implants (CI) are prosthetic devices that restore hearing function in profoundly deaf patients by bypassing damaged parts of the inner ear and directly stimulating the remaining auditory nerve fibers in the cochlea with electrical pulses. To do so, the CI contains a speech processor that plays an important role in converting the original speech signal into electrical stimuli. Traditionally, the processor decomposes the frequency band of the incoming speech into several sub-bands and extracts the envelope of each sub-band for generating amplitude modulated pulses to stimulate the nerve fibers [1].

To realize the spectral analysis in an analog speech processor, band-pass filter designs based on 2nd order filters in the form of log-domain [2-3] and G_m-C [4] filters using CMOS circuits operating in weak inversion have been reported. These filter circuits are successful in terms of power consumption but lack operation that is analogous to a real cochlea. Besides, in conventional speech processors [2-4], the envelopes are extracted by a full-wave rectifier and a low-pass filter that may provide compact hardware implementation, yet their high frequency information is corrupted [5-6].

It was found in [7] that, observing a cochlear nucleus after electrical stimulation, a gammatone function could closely describe the resulting cochlear impulse responses. As a consequence, the gammatone filter has been popularly used in cochlear modeling [8] and speech recognition [9]. Also it has been suggested in [5-6] that, in order to preserve the high frequency information of speech signals, the Hilbert transform should be employed instead of the simple rectifier combined with a low-pass filter.

Recently, partially driven by the motivation mentioned above, a realization of a gammatone filter has been introduced [10]. The design is based on a class-AB log domain circuit using signal splitting and cascaded class-A biquad sections. The filter successfully emulates the pseudo-resonance behavior of the basilar membranes and provides a very high dynamic range of 120dB. This paves the way for high performance bio-inspired analog filter design for new generations of cochlear implants.

In order to develop further, this paper creates a bio-realism of the cochlear channels by combining the gammatone impulse response with the Hilbert transform within a compact frequency selective circuit. The design methodology starts with Laplace transforming the gammatone function into two band-pass transfer functions which represent the real and imaginary signal of the complex gammatone filter. To synthesize the filter, the transfer functions are mapped onto an orthonormal ladder structure which provides good dynamic range, minimum sensitivity to component variations and high sparsity [11]. A sub-threshold G_m-C filter is selected to realize the filter in order to verify the feasibility of the complex gammatone filter at very low power operation.

II. SPECTRAL ANALYSIS IN COCHLEAR IMPLANTS

A. Temporal Envelope and Fine Structure

Applying the Hilbert transform to an incoming speech signal, which is considered a real signal, $x_{re}(t)$, results in an imaginary signal $x_{im}(t)$ which can be combined to create the analytic signal

$$s(t) = x_{re}(t) + jx_{im}(t). \quad (1)$$

In the psychoacoustic literature [5], temporal envelope and fine structure (phase information) are respectively defined by

$$a(t) = \sqrt{x_{re}^2(t) + x_{im}^2(t)}, \quad (2)$$

and $\cos(\phi(t))$, where

$$\phi(t) = \tan^{-1}\left(\frac{x_{im}(t)}{x_{re}(t)}\right) \quad (3)$$

978-1-4244-5309-2/10/$26.00 ©2010 IEEE

is the phase of the analytic signal. The temporal fine structure is critical for speech recognition in background noise and music perception. In [12], it has also been recognized that the temporal fine structure is more important for pitch recognition than the temporal envelope.

B. The Gammatone Auditory Filter Bank

The gammatone filter function describes the impulse responses of the mammalian cochlea and is defined by

$$g(t) = at^{(n-1)}e^{(-2\pi bt)}\cos(2\pi f_c t + \phi)\ ;\ (t>0). \qquad (4)$$

The parameter n is the order of the filter, b is the bandwidth of the filter, f_c is the centre frequency of the filter, a is a constant and ϕ is the starting phase.

In the case of n = 4 and b is 1.019 times the Equivalent Rectangular Bandwidth (*ERB*), (4) can represent the human auditory filter [13]. The *ERB* is a psychoacoustic measure of the bandwidth of the auditory filter at each point along the cochlea. In [14], human data on the *ERB* of the auditory filter has been summarized and can be approximated as

$$ERB = 24.7(4.37 f_c/1000 + 1). \qquad (5)$$

Together, (4) and (5) define the gammatone auditory filter bank. An example of the centre frequencies of 16 cochlear channels and their *ERB* is shown in table I [15].

III. Transformation of Gammatone Filter

A. Laplace Transform of Complex Gammatone Filter

For convenience, we set a=1 and ϕ=0. Then (4) can be modified for a complex tone as

$$g_c(t) = t^3 e^{-2\pi bt}\cdot e^{j\omega t}$$

$$= t^3 e^{(-2\pi bt)}\cos(\omega t) + jt^3 e^{(-2\pi bt)}\sin(\omega t). \qquad (6)$$

Converting (6) into the frequency domain using the Laplace transform properties, we obtain

$$G_{re}(s) = \frac{N_{re}(s)}{D(s)} = -\frac{d^3\left(\frac{s+B}{(s+B)^2+\omega^2}\right)}{ds} \qquad (7)$$

and

$$G_{im}(s) = \frac{N_{im}(s)}{D(s)} = -\frac{d^3\left(\frac{B}{(s+B)^2+\omega^2}\right)}{ds}, \qquad (8)$$

where $B = 2\pi b$ and $\omega = 2\pi f_c$. $G_{re}(s)$ and $G_{im}(s)$ are the transfer functions of the real and imaginary signals, respectively. Note that the denominators of both transfer functions are the same, facilitating a compact hardware implementation which will be illustrated shortly.

To exemplify the case of a centre frequency of 1 kHz and an *ERB* of 132.64 Hz, we have normalized the transfer function as

$$N_{re}(s) = -1.05\times10^{12}s^4 - 3.566\times10^{15}s^3 + 2.441\times10^{20}s^2\cdots$$
$$+4.197\times10^{23}s - 1.457\times10^{27} \qquad (9)$$

$$N_{im}(s) = -2.638\times10^{16}s^3 - 6.722\times10^{19}s^2 + 9.845\times10^{23}s\cdots$$
$$+8.684\times10^{26} \qquad (10)$$

$$D(s) = s^8 + 6794s^7 + 1.781\times10^8 s^6 + 8.389\times10^{11}s^5\cdots$$
$$+1.11\times10^{16}s^4 + 3.372\times10^{19}s^3 + 2.878\times10^{23}s^2\cdots$$
$$+4.413\times10^{26}s + 2.611\times10^{30}. \qquad (11)$$

B. Orthonormal State Space Representation

In order to implement the complex gammatone filter, both real and imaginary transfer functions are mapped onto a state space orthonormal ladder structure. A detailed explanation of the procedure to derive the orthonormal ladder form can be found in [11, 16-17]. The state space description as **A**, **B** and **C** matrices of the example transfer function are given by

$$\mathbf{A}_{re,im} = \begin{bmatrix} 0 & 6201 & 0 & 0 & 0 & 0 & 0 & 0 \\ -6201 & 0 & 778.5 & 0 & 0 & 0 & 0 & 0 \\ 0 & -778.5 & 0 & 6093 & 0 & 0 & 0 & 0 \\ 0 & 0 & -6093 & 0 & 1608 & 0 & 0 & 0 \\ 0 & 0 & 0 & -1608 & 0 & 5788 & 0 & 0 \\ 0 & 0 & 0 & 0 & -5788 & 0 & 3350 & 0 \\ 0 & 0 & 0 & 0 & 0 & -3350 & 0 & 7391 \\ 0 & 0 & 0 & 0 & 0 & 0 & -7391 & -6794 \end{bmatrix}, \qquad (12)$$

$$\mathbf{C}_{re} = [-39.40 \quad 10.99 \quad 4.96 \quad -0.324 \quad -0.158 \quad 0 \quad 0 \quad 0], \qquad (13)$$

$$\mathbf{C}_{im} = [10.95 \quad 39.63 \quad -1.03 \quad -2.46 \quad 0 \quad 0 \quad 0 \quad 0], \qquad (14)$$

and

$$\mathbf{B}^{\mathrm{T}}_{re,im} = [0 \quad 0 \quad 0 \quad 0 \quad 0 \quad 0 \quad 0 \quad 46.50]. \qquad (15)$$

The **A** matrix determines the denominator of both real and imaginary transfer functions. A scaling factor for the whole filter is defined by matrix **B**. It is obviously seen that to realize the real and imaginary outputs, different parameters in matrices $\mathbf{C}_{re}$ and $\mathbf{C}_{im}$ will be used. Therefore, in a practical implementation (G_m-C structure in this case, See Fig.1 in Sec. IV), we can save area and power since all the time constants whose realizations consume most of the total chip area and power can be shared. Unlike other realizations that double hardware to realize real and imaginary transfer functions [18], in this work, only two different sets of transconductors are required.

TABLE I. *ERB* and Centre Frequency of 16 Cochlea Channels [15]

Channels	1	2	3	4	5	6	7	8	9	10	11	12	13	14	15	16
ERB(Hz)	40.89	50.55	62.48	77.23	95.46	118.00	145.86	180.30	222.87	275.49	340.53	420.93	520.31	643.16	795.01	982.71
f_c (Hz)	150.0	239.4	350.0	486.7	655.6	864.4	1122.5	1441.6	1835.9	2323.4	2926.0	3670.9	4591.6	5729.7	7136.5	8875.5

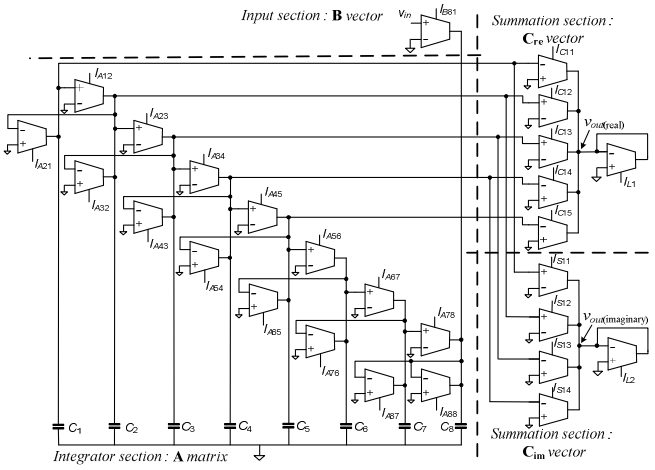

Figure 1. Circuit of the complex gammatone

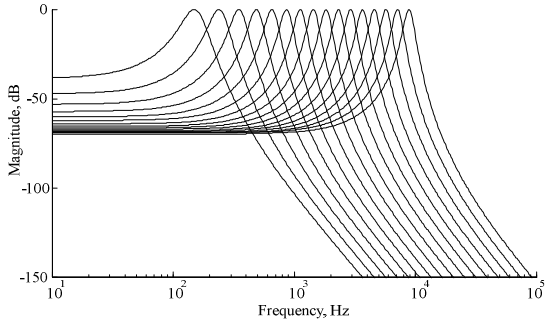

Figure 2. Frequency responses of 16 real gammatone filter channels

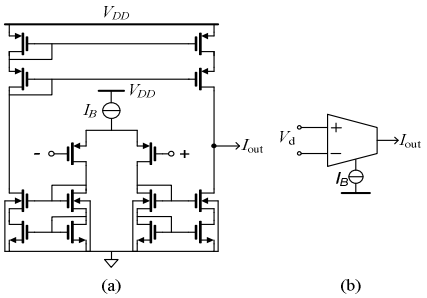

Figure 3. Subthreshold *Tanh* transconductor (a) circuit (b) symbol

IV. CIRCUIT IMPLEMENTATION

Fig. 1 shows the topology of the complex gammatone filter corresponding to the above state-space representation. The frequency responses by using ideal devices (only for the real output) of a 16 channels gammatone filter according to the parameters in table I are shown in Fig. 2.

The circuit design of the filter is based on the G_m-C integrator approach using identical simple sub-threshold differential transconductors as main building blocks shown in Fig.3. The voltage to current relationship of the transconductor is given by

$$I_{out} = I_B \tanh \frac{V_d}{2nU_T}, \qquad (16)$$

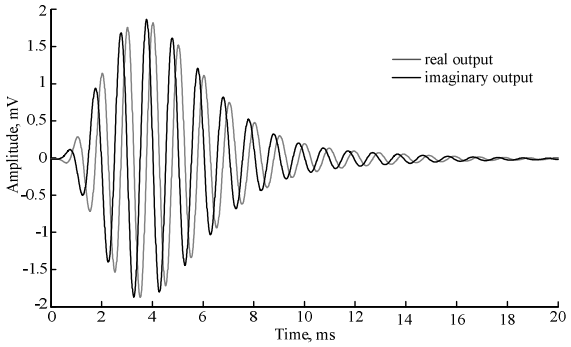

Figure 4. Simulated impulse response at f_c=1kHz

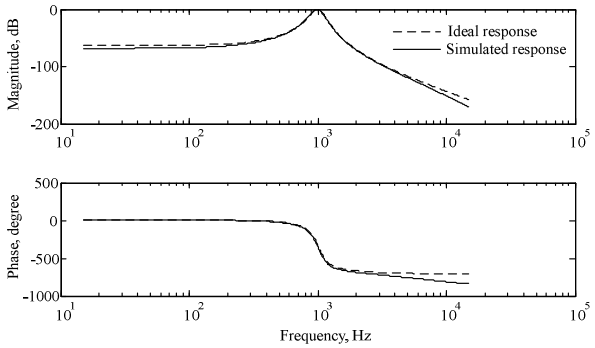

Figure 5. Frequency responses of the real output at f_c=1 kHz

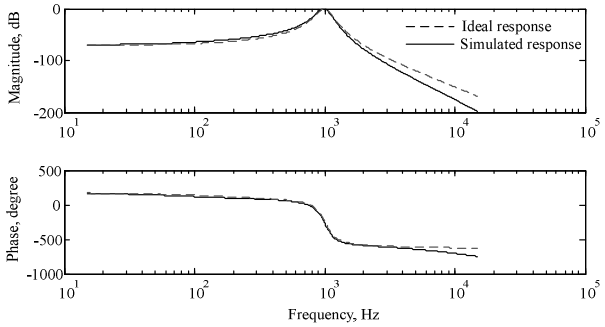

Figure 6. Frequency responses of the imaginary output at f_c=1 kHz

where n and U_T are the sub-threshold slope factor and thermal voltage, respectively [19]. The small signal transconductance, $g_m = I_B / 2nU_T$ can be found from the first term of the Taylor series expansion of (16). The integrator time constants in the **A** matrix are defined by ($\tau = C / g_m$) where C=C_i= 20pF. The bias current of each transconductor is set according to the coefficients in the matrices. The centre frequency and the gain of the filter can be varied by scaling the bias currents of the transconductors of matrices **A** and **B** and **C**, respectively.

V. SIMULATION RESULTS

The concept of the complex gammatone filter was verified in Cadence using RF spectre and AMIS 0.35μm technology. The dimensions equal W/L=6μm/6μm and 6μm/2μm for the PMOS differential pair and all transistors in the cascoded current mirrors, respectively. Supply voltage V_{DD} = 2V and the

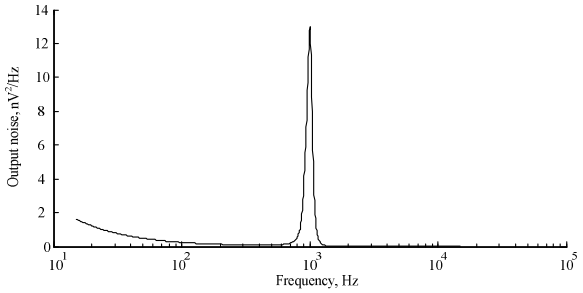

Figure 7. The output noise (PSD)

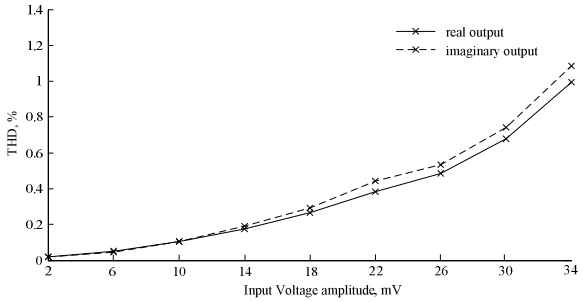

Figure 8. Total harmonic distortion of the proposed filter

common mode voltage reference was set at 1 V. The quiescent power consumption equals 4.71 μW.

Fig. 4 shows the impulse response of the filter at 1 kHz centre frequency by applying a positive pulse signal, with an amplitude of 10 mV and a pulse width equal to 100 μs. The common mode signal has been removed for clarity. The frequency responses of the filter are shown in Fig. 5 and 6 for the real and imaginary outputs, respectively. It is clear that, in the pass-band, the results are close to the ideal case. Fortunately, errors induced from non-idealities of the transconductor occurred mainly in the stop-bands and do not harm the filter's functionality.

The integrated output noise power over the range from 15 Hz to 15 kHz is $2\mu V^2$ and the noise power spectral density (PSD) is shown in Fig. 7. Fig. 8 shows the total harmonic distortion (THD) of the real and imaginary outputs, when sinusoidal inputs signals, ranging from 2 mV to 34 mV, are applied at the centre frequency of 1 kHz.

VI. CONCLUSIONS

The theory and design of a complex gammatone filter for cochlear implant sixteen channels has been proposed in this paper. The key features for speech intelligibility including temporal envelope and the phase information can be extracted from a compact G_m-C poly-phase band-pass filter circuit. This work is considered to be useful for developing the next generation of cochlear implants.

ACKNOWLEDGMENT

The authors would like to acknowledge the financial support for parts of this work by STW, the Dutch Technology Foundation, under project grant 10056.

REFERENCES

[1] F. G. Zeng, S. Rebscher, W. Harrison, X. Sun and H. Feng, "Cochlear implants: system design, integration, and evaluation," *IEEE Rev. Biomed. Eng.*, vol.1, pp.115–142, 2008.

[2] W. Germanovix and C. Toumazou, "Design of a micropower current-mode log-domain analog cochlear implant," *IEEE Trans. Circuits Syst.II: Analog Digit. Signal Process.*, vol. 47, no. 10, pp. 1023-1046, Oct. 2000.

[3] J. Georgiou and C. Toumazou, "A 126-μW cochlear chip for a totally implantable system," *IEEE J. Solid-State Circuits*, vol. 40, no. 2, 430-443, Feb. 2005.

[4] R. Sarpeshkar, C. Salthouse, J.-J. Sit, M. W. Baker, S. M. Zhak, T. K.-T. Lu, L. Turicchia, and S. Balster, "An Ultra-Low Power Programmable Analog Bionic Ear Processor," *IEEE Trans. Bio. Eng.*, vol. 52, no. 4, pp. 711-727, April. 2005.

[5] F. G. Zeng, "Trends in cochlear implants," *Trends In Amplif.*, vol.8, pp. 1–34, 2004.

[6] K. Nie, A. Barco, and F. G. Zeng, "Spectral and temporal cues in cochlear implant speech perception," *Ear and Hearing*, vol. 27, pp. 208–217, 2006.

[7] P.I.M. Johannesma, "The pre-response stimulus ensemble of neuron in the cochlear nucleus," *Proceedings of the Symposium of Hearing Theory*, IPO, Eindhoven, The Netherlands, 1972.

[8] J. L. Flanagan, "Models for approximating basilar membrane displacement - Part II. Effects of middle-ear transmission and some relations between subjective and physiological behaviour," *Bell Sys.Tech. J.*, 1960, 41, pp. 959–1009.

[9] K. Ishizuka, and N. Miyazaki, "Speech feature extraction method representing periodicity and aperiodicity in sub bands for robust speech recognition," *IEEE International conference on Acoustics, Speech and Signal Processing*, Vol. 1, pp. 141-144, 17-21 May 2004.

[10] A. G. Katsiamis, E. Drakakis, and R. F. Lyon, "A Biomimetic, 4.5μW, 120+ dB, Log-Domain Cochlea Channel With AGC," *IEEE J. Solid-State Circuits*, vol. 44, no. 3, pp. 1006–1022, 2009.

[11] D. A. Johns, W. M. Snelgrove, and A. S. Sedra, "Orthonormal ladder filters," *IEEE Transactions on Circuits and Systems I: Fundamentals Theory and Applications*, vol. 36, pp. 337–343, 1989.

[12] Z.M. Smith, B. Delgutte, A.J. Oxenham, "Chimaeric sounds reveal dichotomies in auditory perception," *Nature* 416 (6876), pp. 87–90, 2002.

[13] R.D. Patterson and J. Holdsworth, "A functional model of neural activity patterns and auditory images," *Advances in Speech, Hearing and Language Processing* , (W. A. Ainsworth, ed.), Vol 3. JAI Press, London, 1991.

[14] B. R. Glasberg and B. C. J. Moore, "Derivation of auditory filter shapes from notched-noise data," *Hearing Research*. vol. 47, pp. 103-108, 1990.

[15] M. Slaney, "An Efficient Implementation of the Patterson-Holdsworth Auditory Filter Bank," Apple Computer Corporate Library, Apple Technical Report #35, 1993.

[16] S. A. P. Haddad, J. M. H. Karel, R. L. M. Peeters, R.L. Westra and W.A. Serdijn, "Analog Complex Wavelet Filters," *Proc. IEEE ISCAS*, Kobe, Japan, pp. 3287-3290, 2005.

[17] Ultra Low-Power Biomedical Signal Processing: *An Analog Wavelet Filter Approach for Pacemakers*, S. A. P. Haddad and W. A. Serdijn, Springer, Netherlands, 2009.

[18] X. Zhang and Y. Shinada, "A second-order active bandpass filter with complex coefficients and its applications to the hilbert transform," *Electronics and Communication in Japan*, Part 3, vol. 79, no. 6, pp. 13–22, 1996.

[19] E. A. Vittoz and J. Fellrath, "CMOS analog integrated circuits based on weak inversion operation," *IEEE J. Solid-State Circuits*, vol. 12, no. 3, pp. 224–231, 1977.